4th Annual AIAA/USU Conference
on Small Satellites

at Logan, Utah
August 28 - 30, 1990

OFFEQ - 2

Orbit and Attitude
Flight Evaluation Report

IAI MBT
Systems & Space Technology
ELECTRONICS DIVISION / ISRAEL AIRCRAFT INDUSTRIES LTD

4th Annual AIAA/USU Conference
on Small Satellites
at Logan, Utah
August 28 - 30, 1990

OFFEQ-2

Orbit and Attitude

Flight Evaluation Report

Written by Jerry Wittenstein
Haim Shyldkrot
Michael Grumer
Joseph Komem
Ophir Kubitski
Joseph Kronenfeld

Space Technology Department
MBT Systems & Space Technology
Electronics Division
Israel Aircraft Industries, LTD

Table of Contents

Abstract		3
1.	Introduction	3
2.	Description of Offeq-2	4
2.1	Satellite Systems Description	4
2.1.1	Structure	4
2.1.2	Electrical Power System	4
2.1.3	Thermal Control System	5
2.1.4	Orientation Sensor System	5
2.1.5	Communication System	5
2.1.6	Computer System	5
2.2	Orbital Data & Planning	6
3.	Flight Test Evaluation Results	6
3.1	Summary and Major Events	6
3.2	Orbit and Orbital Lifetime	8
3.2.1	Summary and Current Estimations	8
3.2.2	Uncertainties in the Estimations	8
3.2.2.1	Use of "Best Estimate" Solar Forecast	8
3.2.2.2	Actual Solar Activity	9
3.2.2.3	Attitude Uncertainty of the Satellite	9
3.3	Dynamic Behavior and Orientation	11
3.3.1	Measured Data from TLM	11
3.3.2	Predicted Data from Simulations	11
3.3.3	Estimated Coning Angle Evolution	11
3.4	Thermal and Power Correlations	12
3.4.1	Thermal Data	12
3.4.2	Power Data	13
4.	Systems Reconstruction Approach	14
4.1	Introductory Remarks	14
4.2	Steps in the Procedure	15
5.	Conclusions	16
References		17
Figures		18 - 40
Tables		4,6,41 - 42

Abstract

Offeq-2, Israel's second research and development satellite, was inserted into an orbit of 214 km perigee altitude by 1570 km apogee altitude, on April 3, 1990. Its primary mission was to further demonstrate IAI's satellite technology development and its ground station's ability to track the satellite , send it commands and receive its telemetry.

The Offeq-2 satellite was expected to be on-orbit for about two to two and a half months (60 to 75 days) , and actually was on orbit over three months (97 days). It was expected, due to the dynamic behavior of a spin stabilized satellite under the influence of drag and orbital regression, to enter a period of electrical power loss . This was also expected on Offeq-1 but did not occur due to the rapid development of the coning angle. However, this did occur on Offeq-2, on May the 2nd, as predicted, due to the lack of this rapid coning development. Power did return on May the 8th, and we were able to reconstruct this event successfully.

During the lifetime of Offeq-2, all its objectives were accomplished. The TLM data received provided very valuable information for future use in the planning, designing and operating Israel's future satellites.

This paper reports on the integration of subsystem telemetry data evaluation into a multiple reconstruction of the satellite's performance over several events. This was accomplished using a systems engineering approach, which combined the efforts in several areas: attitude determination via sensor TLM data, dynamic simulations of the attitude and orientation motion, orbital semi-major axis decay, coning angle estimation and electrical power TLM analysis and reconstruction, including analysis of the thermal TLM. We were able to successfully reconstruct the events of the flight including the power outage and resumption.

1. Introduction

The interaction between systems and subsystems and their affected behavior due to environmental factors is amazing;i.e., that one factor or anomaly in a single system will have far reaching effects on many others!

Offeq-2, like its predecessor Offeq-1, was designed as a test flight to further validate the satellite design and the ground support for all future Israeli satellites. This was accomplished very well; however, the differences in the flight results of the two satellites were immense; and nearly all of the differences appear at this time to be due to one factor: the growth or rather the lack of growth of the coning angle!

The goals and objectives of the Offeq-2 flight were to continue augmenting IAI space technology capabilities, to verify two way communications-the downlink (TLM), and the new uplink (TLC) by sending commands to the satellite from the ground station, and to further test the onboard systems operations during exposure to the space environment,

especially the new logic for protecting the computer system against single event upsets(SEU).

2. Description of Offeq-2

2.1 Satellite Systems Description

The Offeq-2 satellite consists of the following systems: Structure, Electrical Power System, Thermal Control System, Orientation Sensor System, Communication System, and the Computer System.

2.1.1 Structure

The configuration is octagonal, whose characteristics are given in the below table 1.

Dimensions	:	Diameter of the Base - 1.2 meters Height - 2.3 meters
Weight	:	174 kg
Telemetry	:	S-Band, 2.5 KB/SEC
Thermal Control	:	Passive, except for the Battery Heater.
Orientation	:	Spin Stabilized, Passive control
Orbital Data	:	210 km Perigee Altitude 1600 km Apogee Altitude 142.2 deg Inclination

Table 1 Offeq-2 Characteristics

The satellite is shown in figure 1, and the basic structure is a truss of aluminum rods, connected by aluminum fittings. The inner shelves are made of the rods and support the satellite systems equipment. The solar arrays are wrapped around the satellite and are attached to the truss, without any load carrying paths. The antenna is at the lower base of the satellite.

2.1.2 Electrical Power System (EPS)

The EPS consists of 16 solar panels, which is the primary power source, a Ni-Cd battery, a relay unit, a power control unit (PCU), and a DC-DC converter (see figure 2).

The mode of operation is by charging the battery via shunt switches controlled by the battery charger. It will short out any excess power from the solar panels, and then charge the battery directly through the main bus. The main bus provides unstabilized voltages to the DC-DC converter which in turn provide stabilized voltage to the rest of the systems. Main bus voltage varies dependent on the battery state of charge.

2.1.3 Thermal Control System

The thermal control system applies both active and passive means to maintain the proper thermal environment.

The system consist of: Multi-layer insulation (MLI) blankets, thermal paints and coatings, radiator, insulators, and conductors, plus a battery active heater.

There are many thermal thermistors located in various places around the satellite.

2.1.4 Orientation Sensor System

These sensors provide the raw information to determine the satellites orientation.

The sensors are: a rate gyro assembly, a magnetometer, and specially arranged solar cells to act as a sun sensor. Additionally, the thermistors provide data to help determine the satellite orientation.

The rate gyro system is a three axis package, and provided the angular rates about the satellites axes. This data is used to generate the spin rate data and the coning angle information as well as the nutation rate.

The magnetometer is located on the top of the satellite and provides data on the satellite orientation with respect to the earths magnetic field.

2.1.5 Communication System

The communication system consist of two redundant transmitters and two redundant receivers, S-Band antenna, and a doubly redundant clock, see figure 3.

2.1.6 The Computer System

The computer system consists of a doubly redundant computer, a doubly redundant TLM data storage unit, power units, and auxiliary units.

The functions are implemented on eight PCB cards.

The functions are: The TLM memory storage switching logic, computer switching logic, switching on and off the gyro package, swapping the transmitters or receivers, and switching on the battery heater. See figure 4 for the block diagram.

2.2 Orbital Data & Planning

The planned orbit is shown below in table 2, showing the key orbital parameters:

Time of Vector	:	4-April-1990
Semi-major Axis	:	7276.1 km
Eccentricity	:	.095682
Inclination	:	143.2 deg
Argument of Perigee	:	72.4 deg
Apogee Altitude	:	1600 km
Perigee Altitude	:	210. km
Mean Anomaly	:	50. deg

Table 2 Major Orbital Parameters

The basic plan was to receive TLM for every opportunity, and to test the uplink system. This was done during communications with the ground station. State vector data was processed during tracking and was used to determine the future communication passes and as the basis for doing orbital lifetime estimations and for the anchor on all our reconstruction efforts.

3. Flight Test Evaluation Results

3.1 Summary and Major Events

The insertion point of the actual orbit was slightly higher than planned, and caused longer AOS times, and a slightly longer on orbit lifetime. The orbital lifetime is discussed later in paragraph 3.2.

The biggest difference noted from the Offeq-1 launch was the smaller initial coning angle, the slightly lower spin rate and the slower growth of the coning angle. This factor led to nearly every known event and anomaly during the Offeq-2 flight. Figure 5 shows both the Offeq-1 and -2 coning histories. See reference 1 for Offeq-1 information.

+P

During Offeq-1 we expected to arrive at sun angles with respect to the solar panels which would result in a loss of power or a power outage after about 30 days. This did not occur, but on Offeq-2 it did occur on about the 30th day, May 2nd. The reason was due to the low coning angle values during this period.

In contrast, on Offeq-2, the coning at the time of the power outage was about 7.6 degrees, whereas on Offeq-1 after the same delta time~ 30 days, the value was approximately 70 degrees. However, the angle between the angular momentum vector and the sun reached the tail;i.e., the central point of the cone of precession, see figure 6, of the satellite at about the same time. This was the crucial factor to the power outage.

This factor lead to several events which did not occur, or actually masked by the large coning, on the previous flight: Rise in temperature in the tail area, dynamic behavior yielded far different drag considerations, the power outage, and return to power. The battery temperature rise was somewhat higher than expected, but this provided a direct clue on the state of battery charge, when its temperature started dropping. This indicated a 70 % or less battery charge. Several temperatures dropped due to the coning situation, causing some divergence in their output.

Until this occurred, all systems operated as expected, and all tests were accomplished satisfactorily. Special test to detect Single Event Upsets (SEU's) were successful, as well as the uplink tests. Analysis of the results from the magnetometer and rate gyro's are still incomplete at this time.

The differences between the two flights can be summarizes as follows:

Systems	Offeq-1	Offeq-2	Effect
- Orientation	Random Tumble [1]	Spin Stabilized [1]	Drag Differences
- Thermal	Slight	Noticeable Rise	None
- Power	No Interruption	Outage for 6 days	Loss of Data

1. Both started spin stabilized but Offeq-1 rapidly tumbled, but Offeq-2 did not.

Significant Events due to differences in coning behavior:

High temperatures at the rear of satellite

Low, cold temperatures at the top of the satellite

Attitude went from spin stabilized to random tumble much later

Power Outage

Only the detection of the SEU's and the computer switch over, which was a improvement from Offeq-1, were not related to the coning, and appear at

this time to be highly correlated to trapped earth radiation, solar storms or cosmic ray radiation.

The tests results are summarized in table 3, and the entries starred are those which occurred in the south atlantic anomaly.

3.2 Orbit and Orbital Lifetime

3.2.1 Summary and Final Estimations:

Offeq-2 re-entered the earth's atmosphere sometime between 21 UTC on the 8th of July to 13 UTC on the 9th of July.

Per the time of this report the date of impact was estimated to be at 2:45 UTC in the morning, with an uncertainty of about .75 hours.

The preflight predicted date was 22-May-1990, with an update due the actual orbit to 25-May-1990, or 57 days with a uncertainty estimate of 48 to 67 days. The reasons for the discrepancy is due to three factors:

1). Use of Best Estimated +/- 2 Sigma Solar activity.

2). The actual solar activity was significantly lower than the Best Estimated nominal.

3). The attitude of the satellite;i.e., the satellite's long axis remained in the orbit plane for longer than predicted.

3.2.2 Uncertainties in the Estimations:

3.2.2.1. Use of the "Best Estimate" Solar Data.

For solar cycles which have not started or have just barely started, then it is reasonable to use 10 to 20 % for the drag coeffient uncertainty, and 75 % for the + two sigma solar activity and 50 % for the - two sigma data. This corresponds to the global solar cycle statistics.

However, after a solar activity cycle is well underway, we can assume a 20 % certainty due to solar activity, thus, the combined uncertainty is about 28.5 %. The reason for using this factor rather than the global statistics, is that one would expect that once the cycle is underway, the uncertainty around it is reduced from the global statistical cycles. This is applicable during the period that the driver factors: attitude, solar activity and tracking data are not yet abundant enough for good estimations. Then, after enough tracking data is available, and that we know the satellite orientation with respect to the wind stream, drag coefficients estimations are made by use of the tracking vectors.

One of the main factors is the method of calculating the uncertainty for the forecasted solar activity, as introduced by NASA. This was a new method of reporting the forecasts of solar activity and the estimate of the uncertainty band associated with it. They no longer normalize previous cycles to an 11 year period. Now they use the 13 month smooth 10.7 cm flux as input to the linear regression model. This method is how the estimates of solar cycle activity is produced. Also, the change shows a higher average solar flux levels. Previously, the spread between the + and - two sigma's to the mean was quite large, but now lies much closer to the "Best Estimate" mean. Thus, the - 2 sigma activity is much higher, therefore closer to our nominal "best estimate" than previous Previously, this case could be nearly 50 % off, now by only 7 %. Figure 7 shows the current solar cycle which is based on the "Best Estimate", versus the next cycle which uses global statistics.

The results of this discussion is that the forecast of lifetime using the - 2 sigma "Best Estimate" flux provides a much shorter delta lifetime than previously used methods. This is not a criticism of the method, since it did a good job in making the spread in the flux forecast consistent with the use of a better defined mean. Plus, the actual is still much, much closer to the best estimate low activity data than to the global case. Nevertheless, the actual solar activity did turn out to be somewhat lower than the earlier forecasts, as is discussed below.

If we had used the global solar cycle statistics, the 2 sigma long lifetime would have been 27-July-90 (also using bias discussed below).

3.2.2.2 Actual Solar Activity

Additionally, the solar activity is significantly lowers the "best estimate". We used Sept-89 forecasts as a basis for our estimations, and there was about 15% to 20 % difference between the current monthly data and the solar activity used for our preflight predictions;i.e., the monthly averages are over 20 % lower than the predicted 13 month averages.

Although, it is not known now, the current monthlies and thus the expected 13 month average, may be below the "Best Estimate" - 2 sigmas! To illustrate the shift, see the attached figure 8. This shows the rather sudden shift in solar activity to values below that of the "Best Estimate" - 2 sigma.

3.2.2.3 Attitude Uncertainty of the Satellite

There is only one way of getting around the problem of predicting the lifetime: to perform drag reconstruction by use of the tracking data. Then to apply to resulting biases to the ballistic factor, for use in subsequent predictions. Plus, to continually update the basis for shifts in the attitude or changes in in atmopheric density. Only after six and a half months, can we completely be sure of the solar activity effect.

Applying this procedure to the lifetime estimates, we found that the results very interesting. As expected, this method applied to the drag force in our simulations provided a very close fit in the reconstructed state vectors and the actuals.

Starting near the beginning we found the following:

For the portion between April 4th and about mid May, I found that the ballistic factor was nearly reduced by about 40 %!!

Next it is noted that in mid June the difference in drag between the predicted and actual state vectors was lower by only about 13.1 %. Figure 9 shows the reconstruction of the semi-major axis based on the June 25th state vector.

However, since the expected delta due to the solar activity will probably be closer to 20 %, which is about half of the bias applied to the ballistic factor. Thus, some other factor in the ballistic factor needed investigation. One that could cause higher than the probable solar flux could cause and later less that this.

Looking for an additional factor other than the solar activity requires the investigation of the ballistic factor.

BF = M/Cd*A & Density = f(F10.7, ap)

Since the force due to drag is a function of the drag coefficient, the satellite cross-sectional area, the atmospheric density and its mass, there is only one major unknown that can be deduced, that is, the cross sectional area. Plus it fits the bill; it can cause reductions and additions to the drag force at different times. It should be pointed out that in the current solar activity models, that it is not clear that we can really separate the density from the ballistic factor and also it is not clear if we truly can separate the Cd from the cross-sectional area! See references 2 and 3. By examining the angle between the angular momentum vector and the normal to the orbit plane, we see that there is a trend to being more perpendicular to it and thus the average cross sectional area will increase with time. This effect was mostly cancelled out on Offeq-1 due the early, large growth of the coning. This is shown quite nicely in figures 10 and 11.

The best fitted data was 40 % of the expected drag till about May 15th, than varied between 86 % to 95 % as the attitude started varying. Applying these factors to the simulation, or better a reconstruction, yields an estimated or reconstructed impact date of 9-July-1990. Table 4 shows the factors used for the reconstruction.

A more thorough reconstruction was made using the last several vectors available, the results are shown in figure 12, and the map of the last revs, with the best estimated decay point, as shown in figure 13.

3.3 Dynamic Behavior

3.3.1 Measured Data from TLM Processing

Data was regularly received from the orientation sensors, and processed. This data is shown in table 5, and consist of the coning angle, angle between the sun and the angular momentum vector, plus the location of the angular momentum vector in the inertial frame(x to vernal equinox, z along North pole) in terms of declination and right ascension.

3.3.2 Predicted Data from Simulations

This data was further used in a dynamic simulation of the satellite attitude, which then predicts the future attitude and orbital conditions. The figures 14 to 15 gives the result of a typical forecast and how it compared to actual data received later. This simulation and the electrical power simulation provided the times to expect the power outage period.

3.3.3 Estimated Coning Angle Evolution

Our only previous "hands on" experience with coning was from Offeq-1. That, as was shown earlier, grew quite rapidly. However, we assumed that since the satellites are very similar, then the coning characteristics should also be quite similar.

In order to understand the coning process that occurred on Offeq-1, a dynamical model was developed to simulate the nutation growth in a simple spinner. The simulation includes the essential elements to account for the internal energy dissipation in the Offeq satellites.

The model developed simulates the increase in tranversal angular velocity up to the flat spin and the corresponding decay of the spin rate, in the body axes of the satellite. It simulates a simplified sloshing mechanism in one or multiple tanks, compare this with reference 5.

The model uses the following equations of motion:

$$(1) \quad \dot{p} = -(1/Iz)[Il(q\dot{e} - r\dot{q})]$$

$$(2) \quad \dot{q} = -1/Ix[(Iz - Iy)rp + I^{1}(\ddot{a} - \dot{e}p)]$$

$$(3) \quad \dot{r} = -1/Iy[(Ix-Iz)pq + Il(\ddot{e} + \dot{a}p)]$$

$$(4) \quad \ddot{a} = -1/Il[2Fd\dot{a} + Ilpa^{2} + 2Ms(R^{2} + Zc^{2})\dot{q}]$$

$$(5) \quad \ddot{e} = -1/Il[2Fd*\dot{e} + Ilpe^{2} + 2Ms(R^{2} + Zc^{2})\dot{r}]$$

Where $I1 = 2MsR2$

$\dot{p}$ = spin axis angular velocity

$\dot{q}$, $\dot{r}$ = transversal angular velocities

a, e = the imaginary angular displacement coordinates of liquid movement in the xz and yz planes.

Fd = the linear coefficient of viscous friction.

Ms = the lumped liquid mass.

R = the gyration radius of Ms.

Ix, Iy, Iz = the satellites principal moments of inertia.

Zc = the distance parameter

The simulation fits the conservation of the satellite models angular momentum to about .1 % up to flat spin conditions. Also, for Zc = 0, and with through the range of nutation angle to 90 degrees, flat spin, the kinetic energy loss of the satellite and the liquid was equal to the energy dissipated within the viscous dampers.

Up to nutation angles, THETnut, of 15 degrees, the dynamical process fits nicely with the energy sink approach,

$$THETnut2/THETnut1 = Exp(del\ t/Taunut)$$

with the Taunut, time constant of the coning angle growth, increasing slowly.

This can be written in the form:

$$(6)\ Taunut = Iz[(Iz/Ix)^2 -1]*Wz^2*THETnut^2/ Edissipation.$$

Where E is the kinetic energy.

This was than applied to the telemetry received from Offeq-2, with 142 < Taunut(Revs) < 184, with THETnut increasung to about 7.6 degrees.

Adjusting, the full model for the different initial conditions of Offeq-2, similar forecasts was made based on the empirical conditions of both satellites. This is shown below in figure 16 and 17 for Offeq-1 and 2 respectively.

3.4 Thermal and Power Correlations

3.4.1 Thermal Data

Mostly the thermal data was as expected high in the aft section and cold in the front section. rise and drop in temperature as the sun entered the rear of the satellite did indeed occur as originally expected. Figures 18 & 19 show the front and aft cover temperatures of the satellite.

The only real problem was the temperature of the magnetometer, shown in figure 20, got quite cold and exceeded the recommended operating limits,

and this is exhibited in the effect on magnetometer reading processed to yield the coning angle, which is dropping when it should be continuing to rise.

However, an important drop in temperature occurred when the battery temperature dropped just prior to the power outage. This data gave us the clue that the battery state of charge had dropped to 70 % or below. When fed into the EPS simulation, it gave good initial conditions for estimating the power balance situation which allowed pretty accurate estimations on the power outage and return, especially in the reconstruction of the return to power.

3.4.2 Electrical Power Data

The above discussion indicated the state of the battery charge and the overall balance prior to the power outage. However, up to the time of the drop in battery temperature, the orbit by orbit power balance situation was as expected, and performed as designed.

The voltages and currents for the mission are shown in figures 21 and 22, which also show the drop in voltage that occurred due to low charge currents.

The simulation reconstructed the EPS balance for the power outage by use of the forecasted attitude from the above mentioned dynamics simulation and the expected temperatures and sun angles on the solar power. Also, the measured voltages and state of charge at the times of the battery temperature drop were input, and the simulation then estimated the times of the loss and return of power within hours.

The electrical power outage occurred during the night between 5/1/90 and 5/2/90, as the result of a low sun angle with respect to the solar panels. As the satellite slowly changed its orientation, the sun angle increased and the electrical power was resumed on 5/8/90.

A computer simulation of the EPS was done for a period of two weeks starting from 4/26/90, in order to examine the event of power outage.

3.4.2.1 Description of Simulation

The simulation consists of three modules:

- Solar panels simulation:

It computes the work point on the I.V. curves of the solar cells according to their characteristics, their voltage, their temperature and the sun angle. The output of this module is the current (and power) generated by the solar panels as function of time.

- Battery simulation:

Consists of voltage profiles as function of charge/discharge current, battery temperature and battery state of charge/discharge.

- Electrical power consumption:

Consists of a table of all the power consumptions of the users as function of time.

The input to this simulation was the sun angle, the coning angle of the satellite, the length of satellite day, length of eclipse, battery temperature and average temperature of the solar panels.

3.4.2.2. Results

Figure 23 describes the simulated electrical balance for the period between 4/26/90 and 5/10/90. The upper part consists of two graphs: The power generated and the power consumed. The power generated varies from 120 watts to 155 watts, at time zero. The reason for the power variations is due to the sun angle variation with respect to the solar panels due to the satellite coning. The power generated drops to zero during the eclipse.

The power consumed is given one value during the satellite day (51 watts) and a lower value during eclipse (48 watts).

The lower graph describes the state of charge in the battery. The battery is discharged during eclipse and charged during the day. However, at time zero, the power generated is not sufficient to fully charge the battery during the day, thus causing a slow overall discharge.

The power generated changed slowly as the sun angle lowered and coning increased, until finally, the battery was fully discharged on 5/1/90 at 17:00 (see figure 23).

The battery's full discharge lasted until 5/8/90 after 12:00, even though the power available was adequate for the previous two days. The reason for the battery not being charged even though the solar panels generated an average of 100 watts on 5/6/90 lies in the end of charge mechanism. The power control unit (PCU) controls the end of charge by reducing the charge current as the battery voltage increases due to increase of state of charge. Since the battery temperature was much higher than planned, the PCU stopped battery charge much too early. Thus the battery charge resumed two days after the power generated was sufficient. Once the temperature dropped on the battery, as discussed above, we knew the charge had dropped to the 70 % level.

4. Systems Reconstruction Approach

4.1 Introductory Remarks

The approach described here and alluded to above is not unique but rather is the classical or traditional approach used in the space business for years, although not always with complete success. However, in the case of Offeq-2 it worked as it should, and usually does when the data is known. It simply consists of the integration of the efforts of several disciplines into a complete picture of what occurred. See figure 24 for the procedure and processes used.

The major factor in the events which occurred on Offeq-2 was the slow growth of the coning angle with respect to Offeq-1. Given this condition and the fairly predictable precession of the satellite in the the orbit plane and the even better known position of the sun, the results then are as expected. This, however, required the combining the work of several areas:

System Dynamic Simulation- which forecast and reconstructed the satellites orientation history and orbital motion.

Electrical Power Simulation- which predicted and reconstructed the power balance, required versus available, as a function of time.

Attitude Determination-which provided the measured attitudes as input to the satellite dynamic simulation, from the rate gyro's and magnetometer, which yielded the coning angle and its precession rate and the attitude of the satellite with respect to the environment.

Orbit Determination- which provided the orbital decay parameter, the semi major axis with time, and provided valuable drag information.

4.2 Steps in the Procedure

The procedure was as follows:

TLM data was processed yielding satellite orientation data, temperatures, power system currents and voltages, and given a preliminary check against red-lines. Concurrently, tracking data was processed and orbital state vectors generated. Solar activity data was updated as fast as possible.

The measured orientation data was supplied to the Dynamics Simulation, which then after generating the complete dynamics forecast, checked the orbital data against measured state vectors.

Then the best available solar data was input to the simulation, and rechecked the measured orbital data against the predicted. Then the Cd*CA was varied until the orbital data matched, and also the attitude data matched. This is somewhat iterative, but seems to work well. After the attitude data is fit as well as possible, it is then possible to evaluate the Cd or biases in our models.

After a good fit is available, then the Electrical power simulation is fed the data on orientation angles and orbit to construct the environmental conditions for the the solar panels and the battery. This was then matched against the EPS currents and voltages and biases in the preflight or ground testing determined, and the biases in the simulation.

This data and approach was used to generate the results shown above for orbital lifetime ands the times for power off and on again. Since the match was close during the mission and as evaluated post mission, the approach was successful in reconstructing the anomalies noted, the occurrence of the key events and determining pretty successfully the lifetime of the satellite.

5. Conclusions

The Offeq-2 mission not only accomplished its goals, but revealed many important factors for future planning and design of IAI's satellites:

Design for solar activity uncertainties,
Protect the Satellite computer against radiation,
Be prepared for power outages and their effects.

References:

1. OFFEQ-1, Preliminary Flight Evaluation Results, Wittenstein and Barlev, February,1989. 31st Israel Conference on Aviation and Astronautics , February 1989

2. Skylab Mission Report: The Final Days, Thomason, Chubb, Kennel, Little, Wittenstein, ..., August 1979-NASA Report

3. Skylab Reentry Report - July 10 and 11 1979, Wittenstein, Little Dreher, August 1979

4. Skylab Orbital Lifetime Prediction and Decay Analysis, Dreher, Little and Wittenstein, November 1980, NASA Technical Memorandum 78308

5. Stabilization and Control of Spacecraft, A.E. Bryson, AAS Guidance and Control Conference , 1983, Vol 44, AAS 83-087

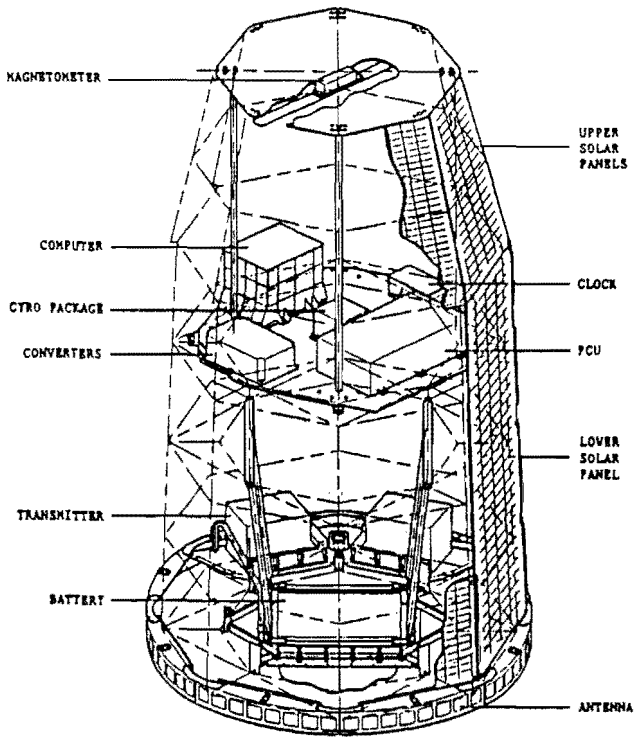

Figure 1. OFFEQ-2 - General View

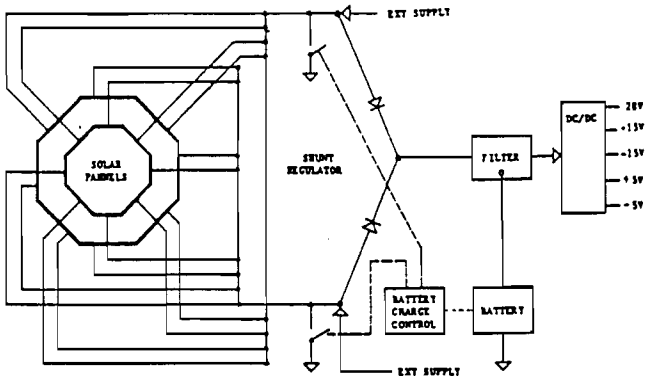

Figure 2. Electrical Power System - Principle of Operation

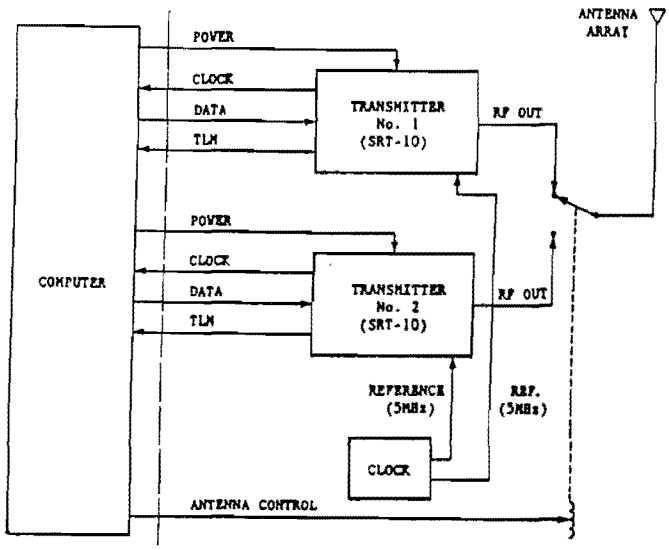

Figure 3. Communication System - Functional Block Diagram

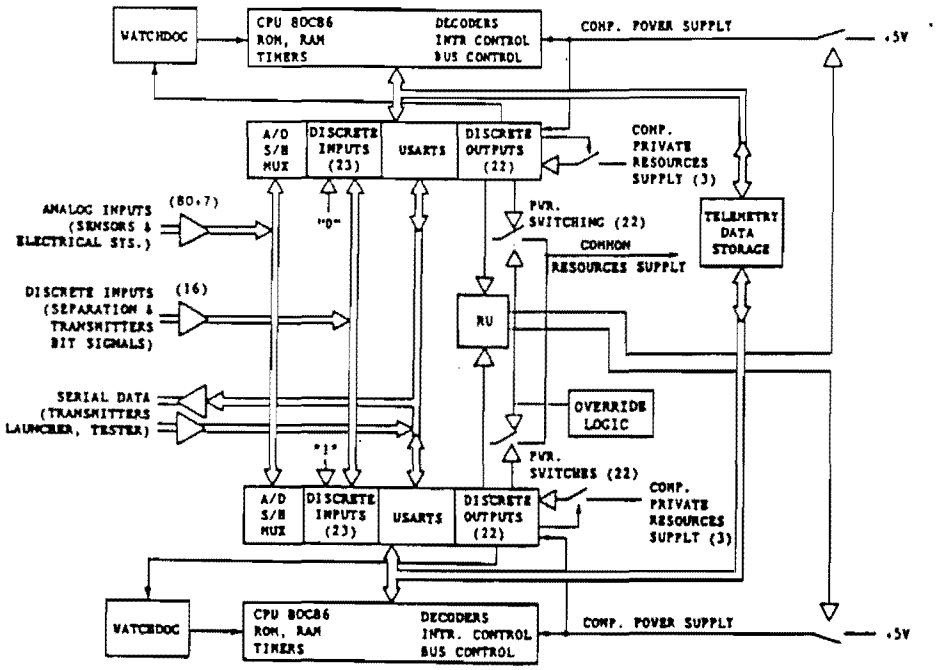

Figure 4. Computer System - General Block Diagram

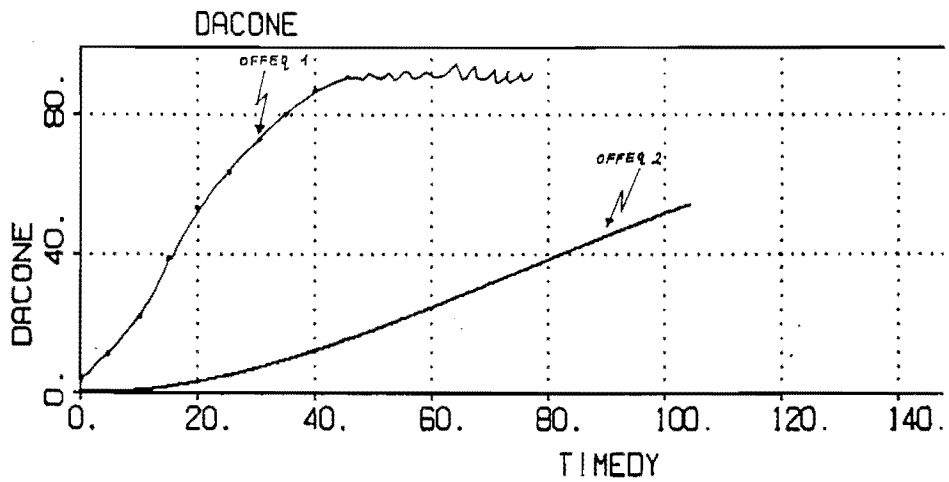
DACONE
OFFEQ 1
OFFEQ 2
DACONE
0.
40.
80.
0.
20.
40.
60.
80.
100.
120.
140.
TIMEDY

Figure - 5

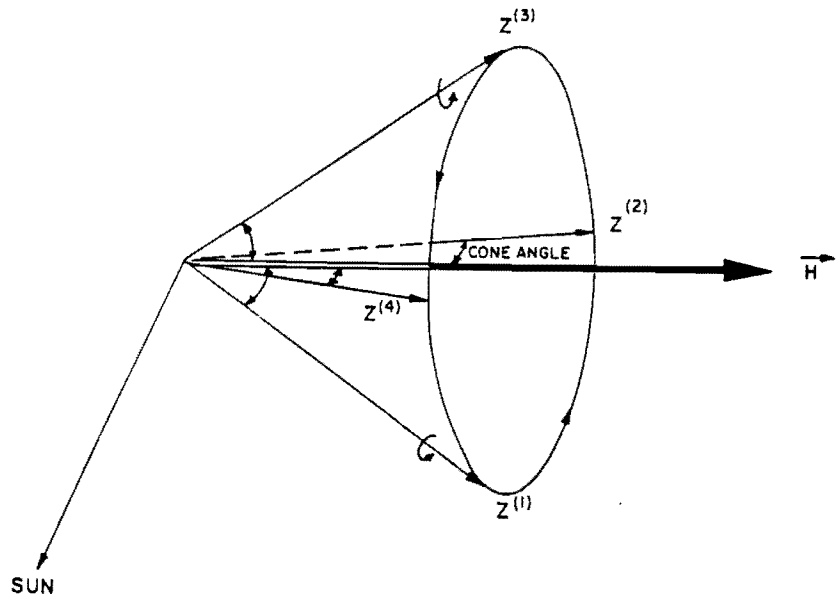

NOTES :

$Z^{(1)}$ IS Z - AXIS IN PLANE OF $\vec{H}$ & SUN

$Z^{(2)}$ " " " " " " 90° TO $\vec{H}$ & SUN

$Z^{(3)}$ " " " " 180° FROM $Z^{(1)}$

$Z^{(4)}$ " " " " " " $Z^{(2)}$

CONE ANGLE

Figure - 6 Geometry of Satellite Coning Angle Movement

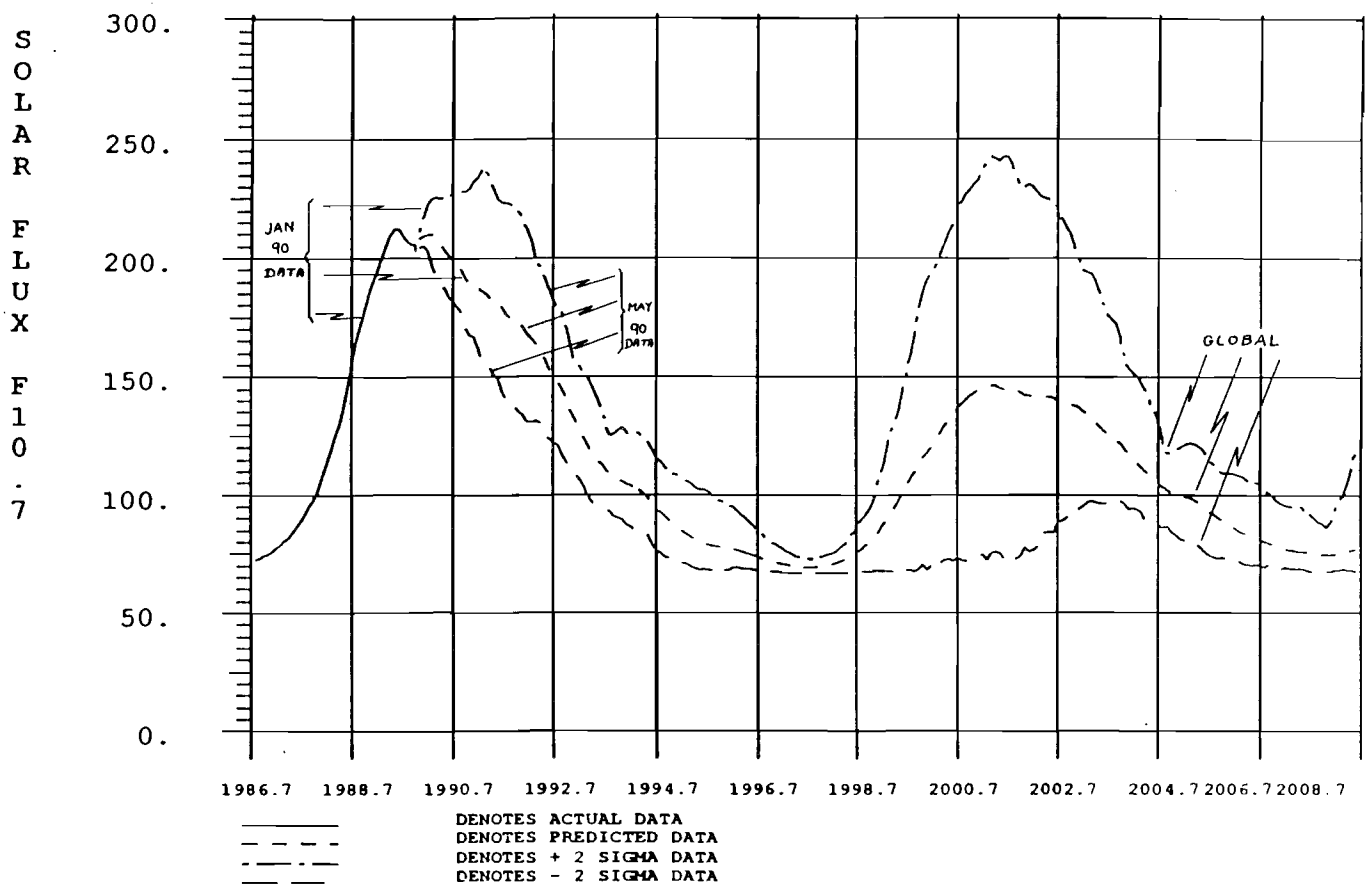

1 COEFFICIENT LINEAR MODEL USING CYCLE 1 THROUGH 21
PREDICTING CYCLES 22 AND 23 FROM POINT 39

Figure 7 Long Range Estimates of Smooth 10.7 cm Flux for Cycles 22 and 23

Solar Cycle 22 Compared to Previous Cycles

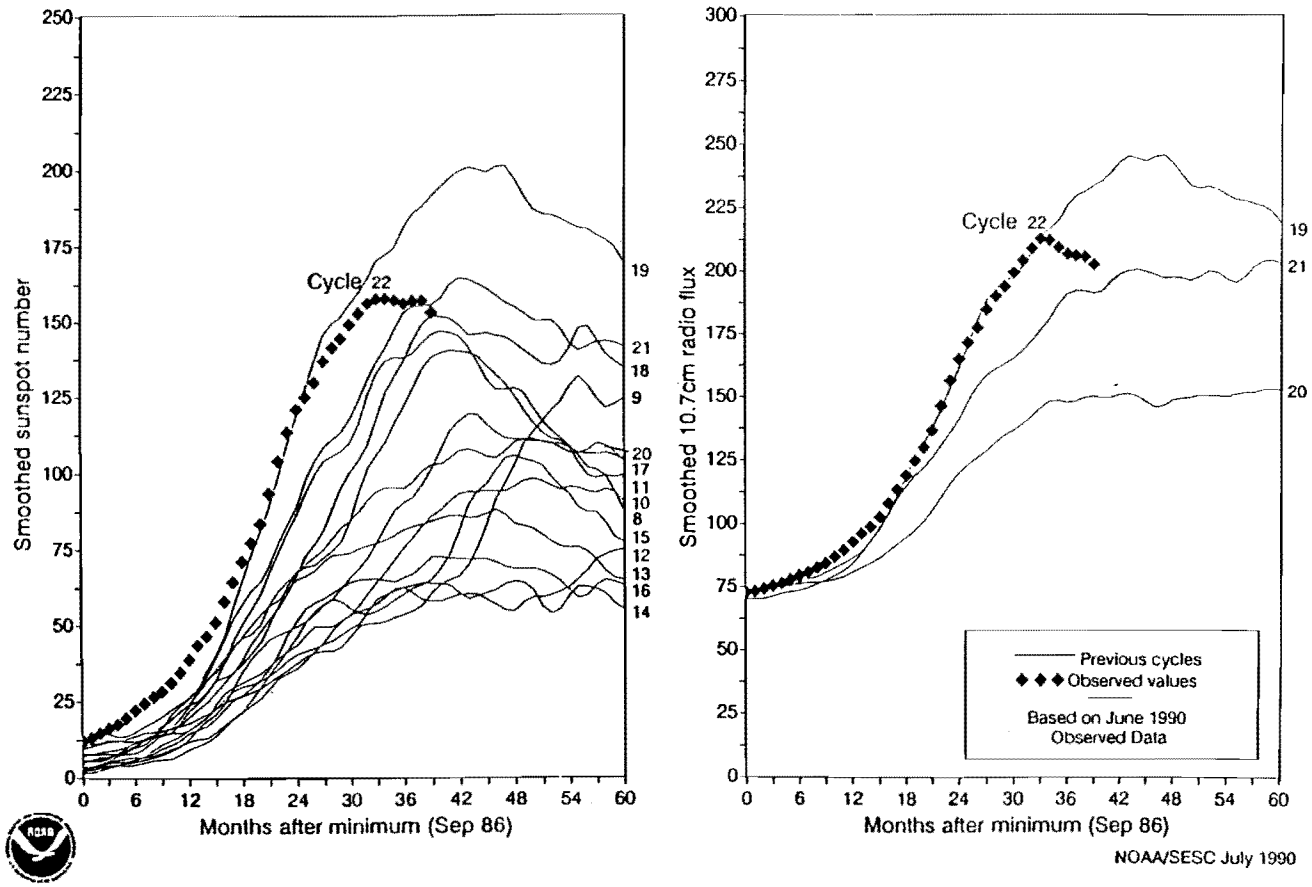

Figure - 8

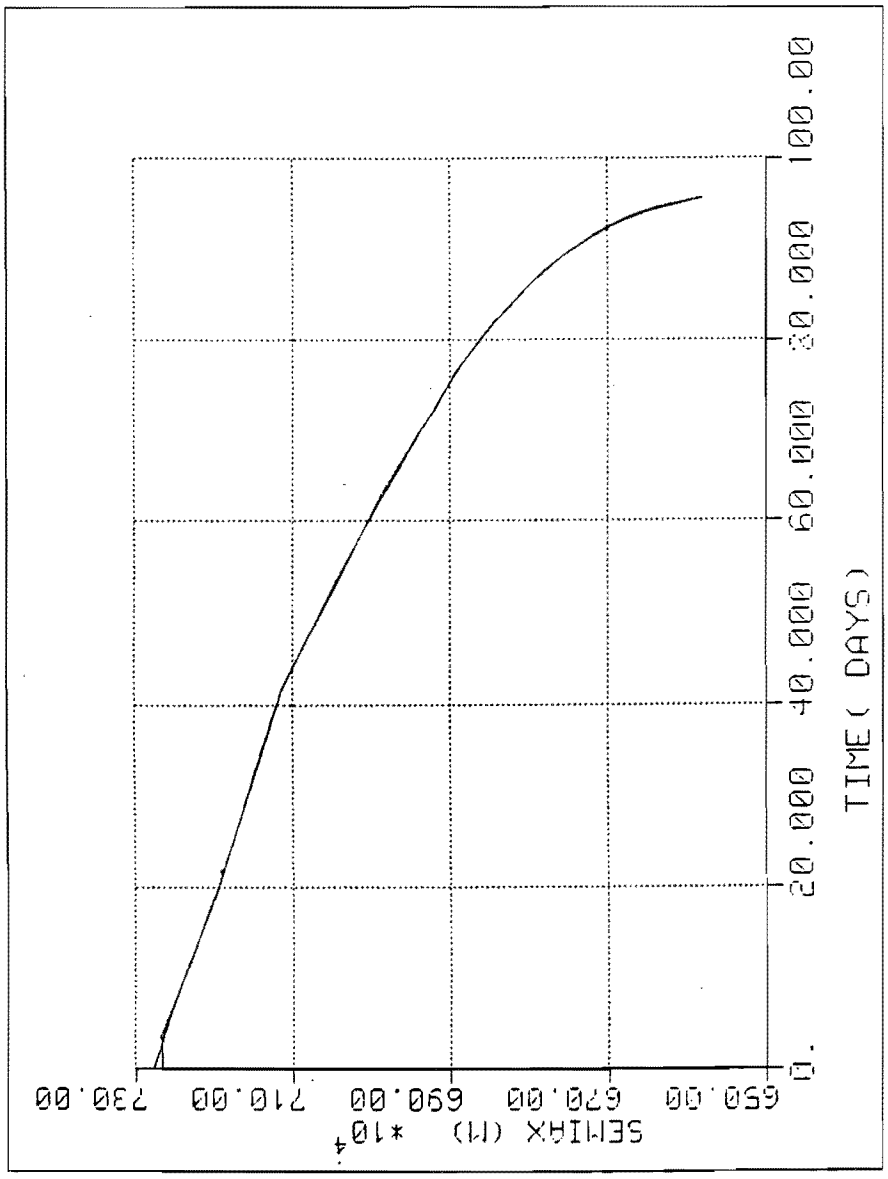
SEMIAX (M) *10^4
650.00
670.00
690.00
710.00
730.00
0.
20.000
40.000
60.000
80.000
100.00
TIME (DAYS)

Figure - 9

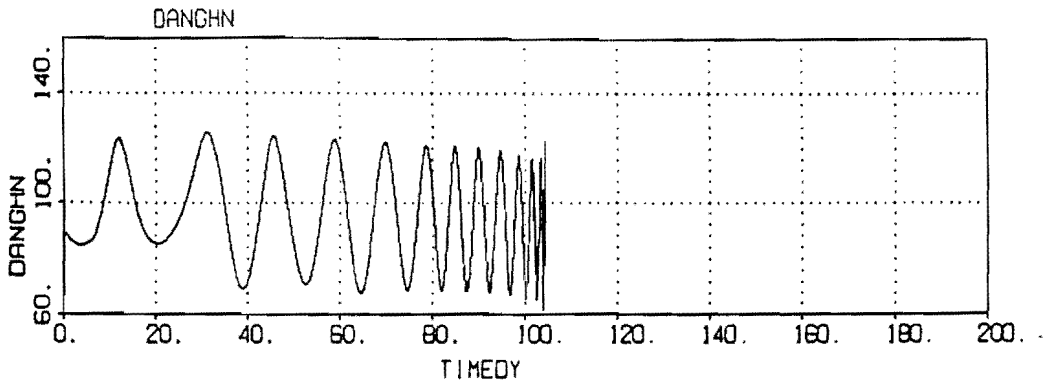

Figure -10

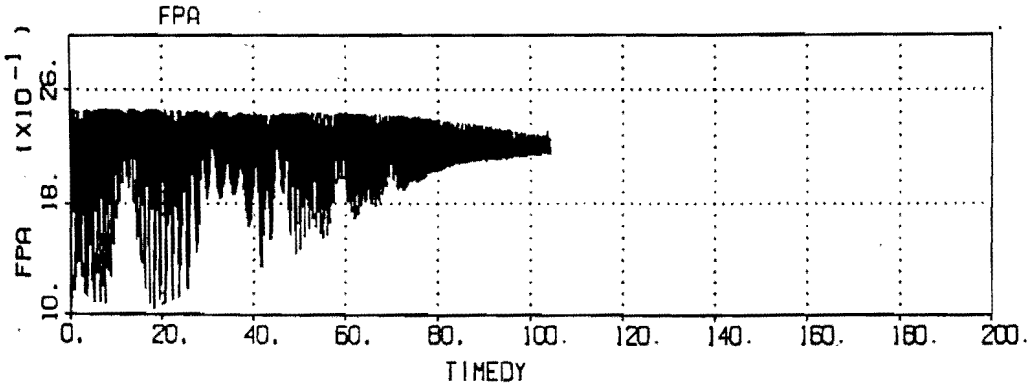

Figure - 11

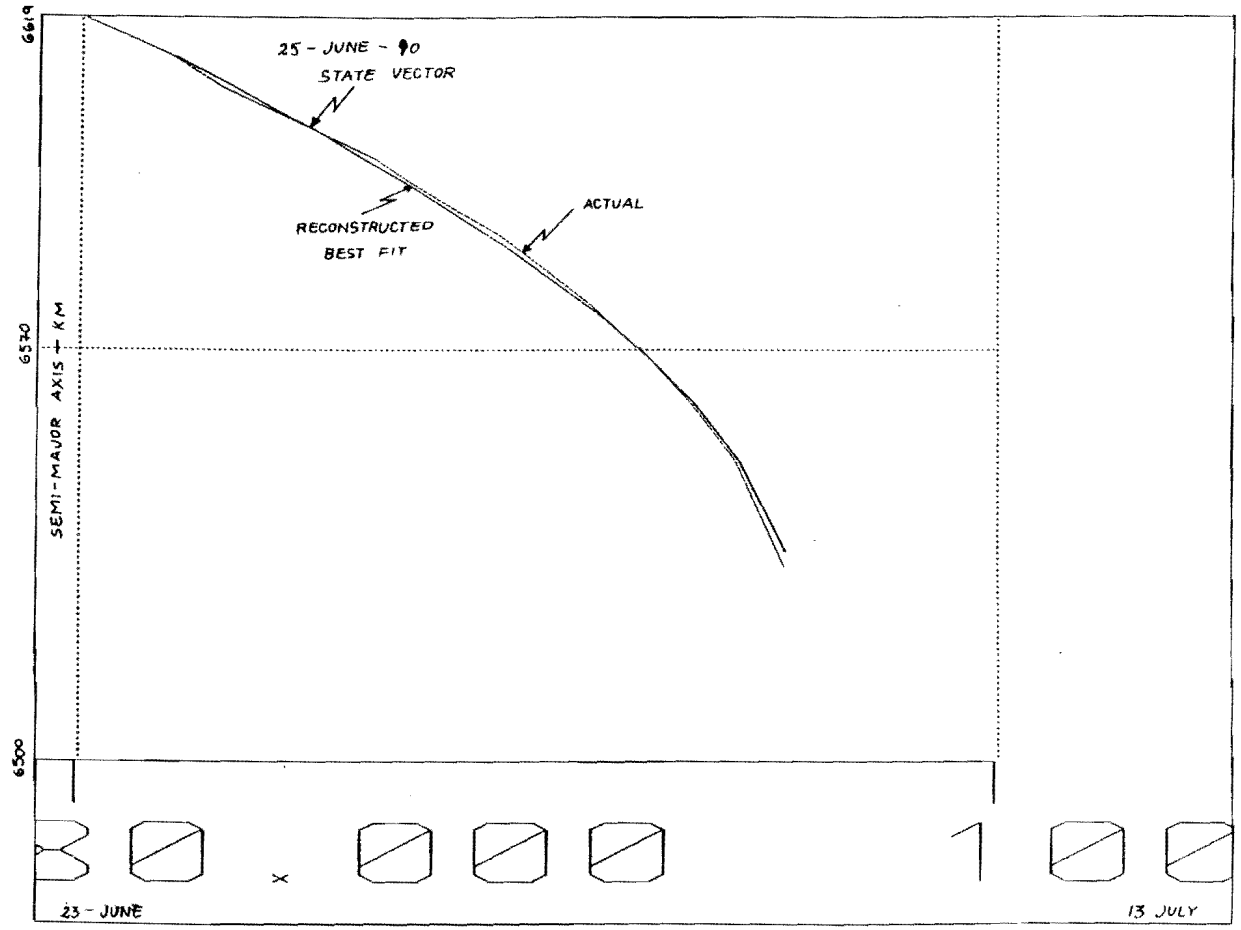

Cd FACTOR
25 JUNE 8.69
28 JUNE 8.45

FIGURE 12: ZOOM - SEMI - MAJOR AXIS
ACTUAL VS RECONSTRUCTION

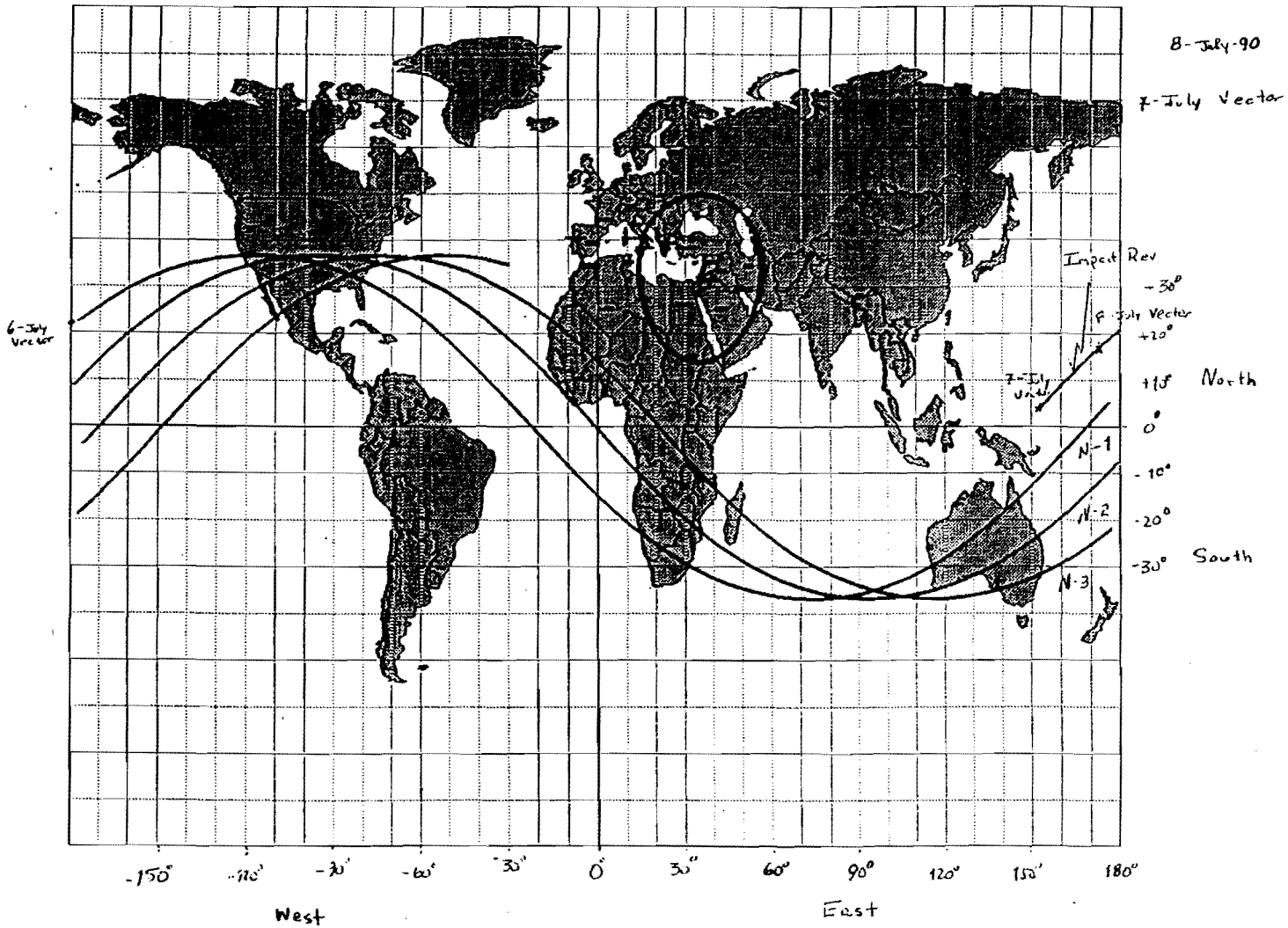

FIGURE 13: Offeq 2 Re-entry Rev (-3)

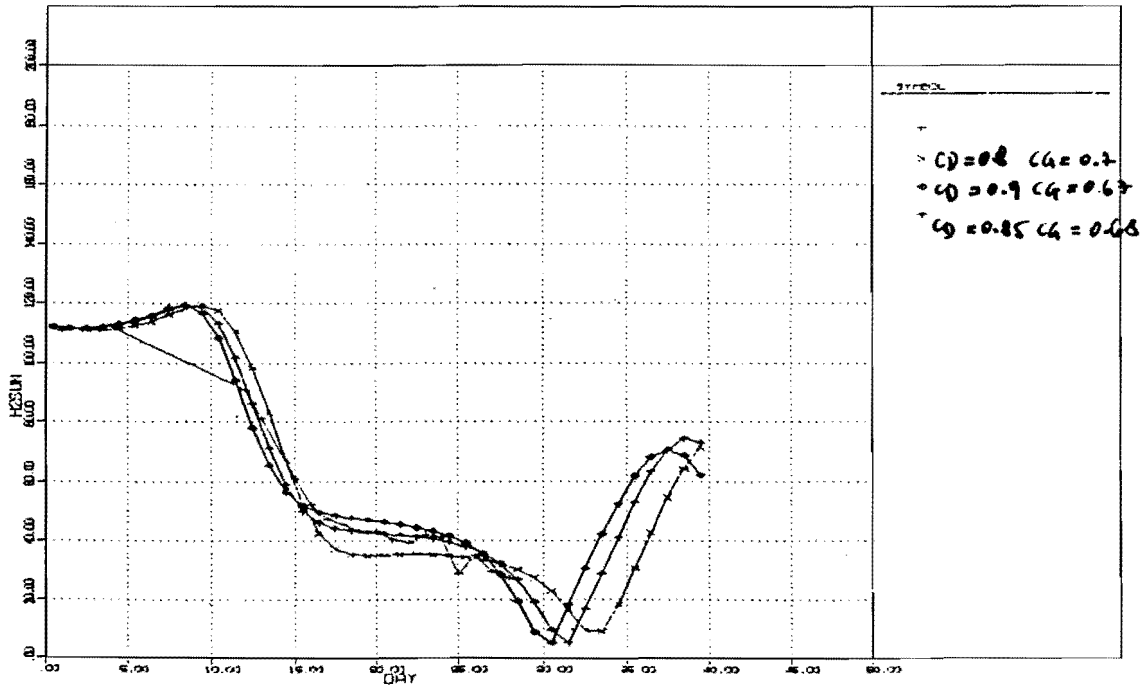

Figure - 14

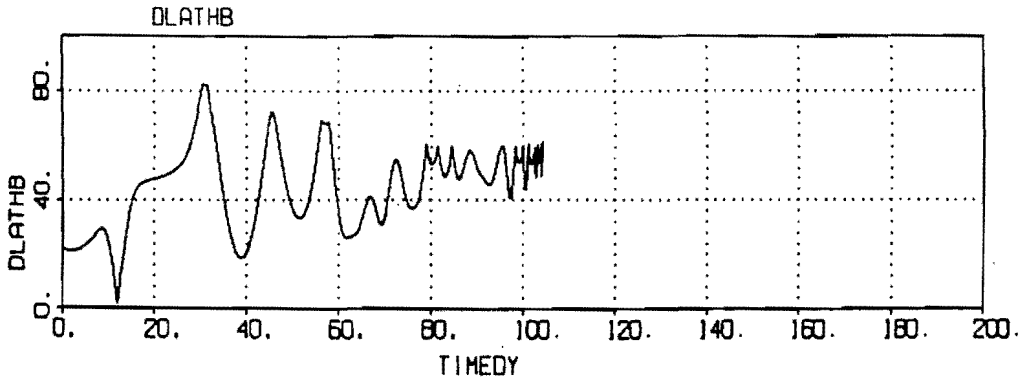
DLATHB
DLATHB
0.
40.
80.
0.
20.
40.
60.
80.
100.
120.
140.
160.
180.
200.
TIMEDY

FIGURE - 15

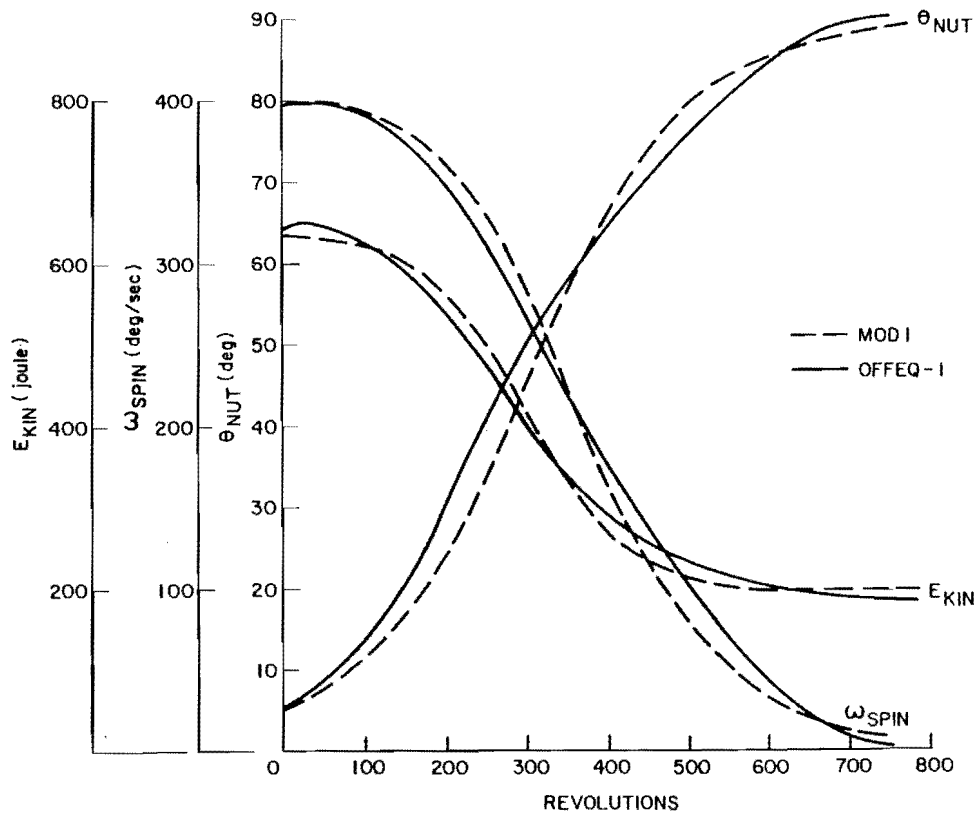

FIG-16 CONING EVOLUTION OFFEQ-1

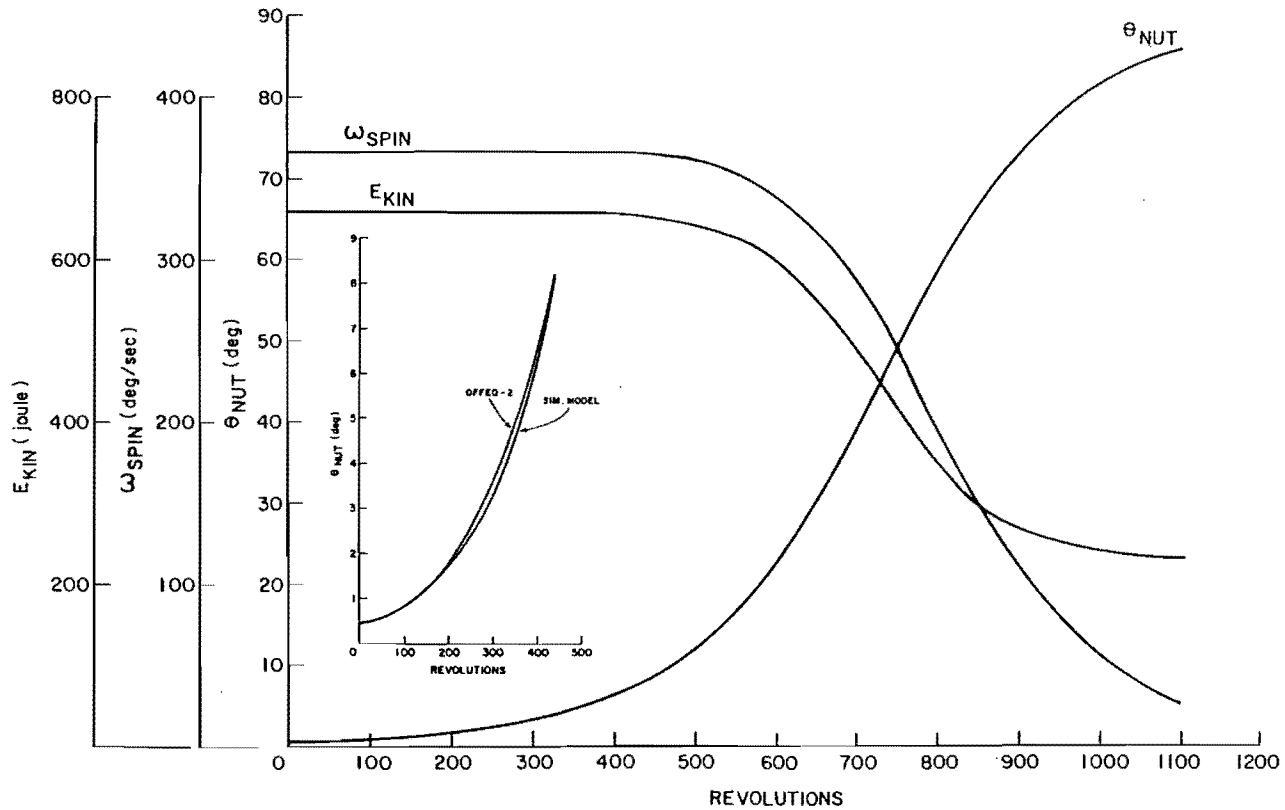

FIG - 17 CONING EVOLUTION OFFEQ-2

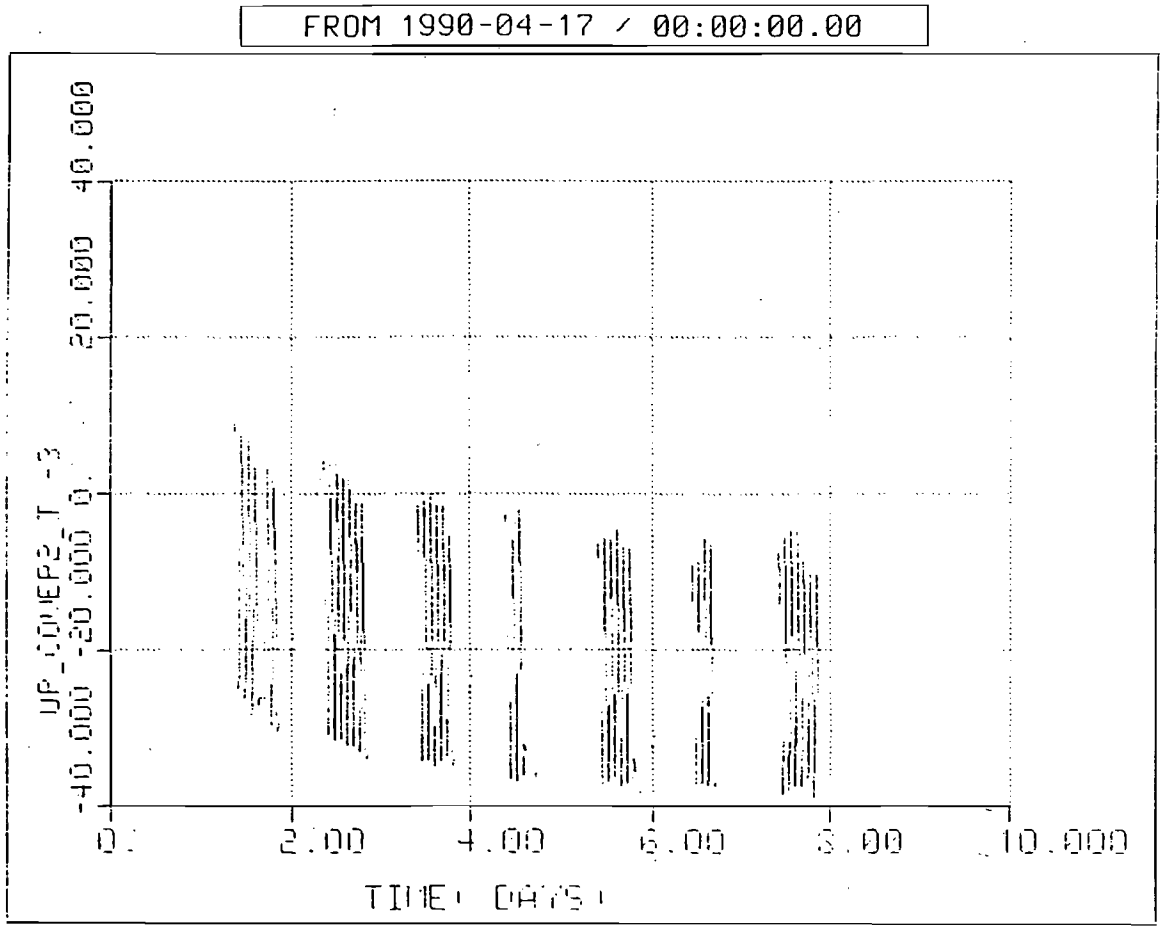
FROM 1990-04-17 / 00:00:00.00
UP_COMEP2_T -3
40.000
20.000
0.
-20.000
-40.000
0.
2.00
4.00
6.00
8.00
10.000
TIME, DAYS

FIGURE - 18

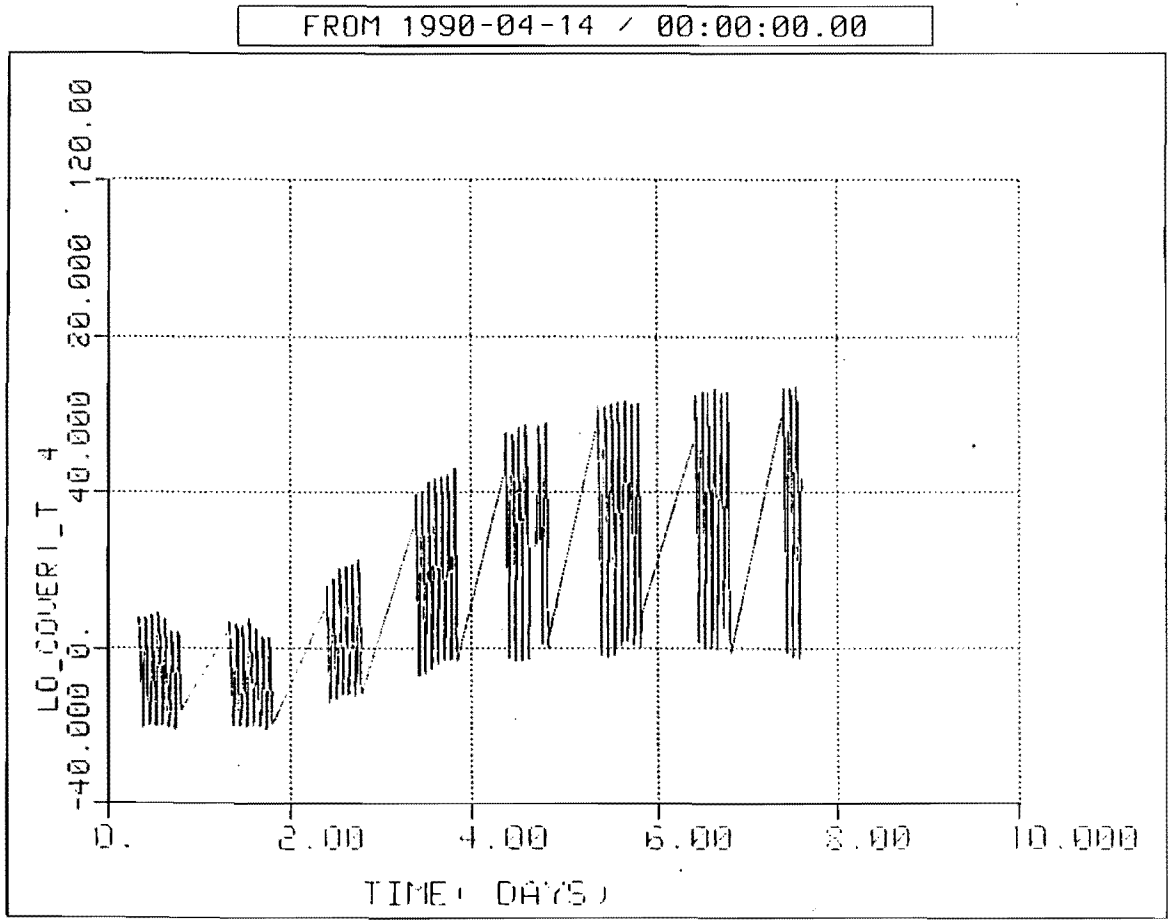
FROM 1990-04-14 / 00:00:00.00
LO_COVERI_T_4
-40.000
0.
40.000
80.000
120.00
0.
2.00
4.00
6.00
8.00
10.000
TIME(DAYS)

FIGURE - 19

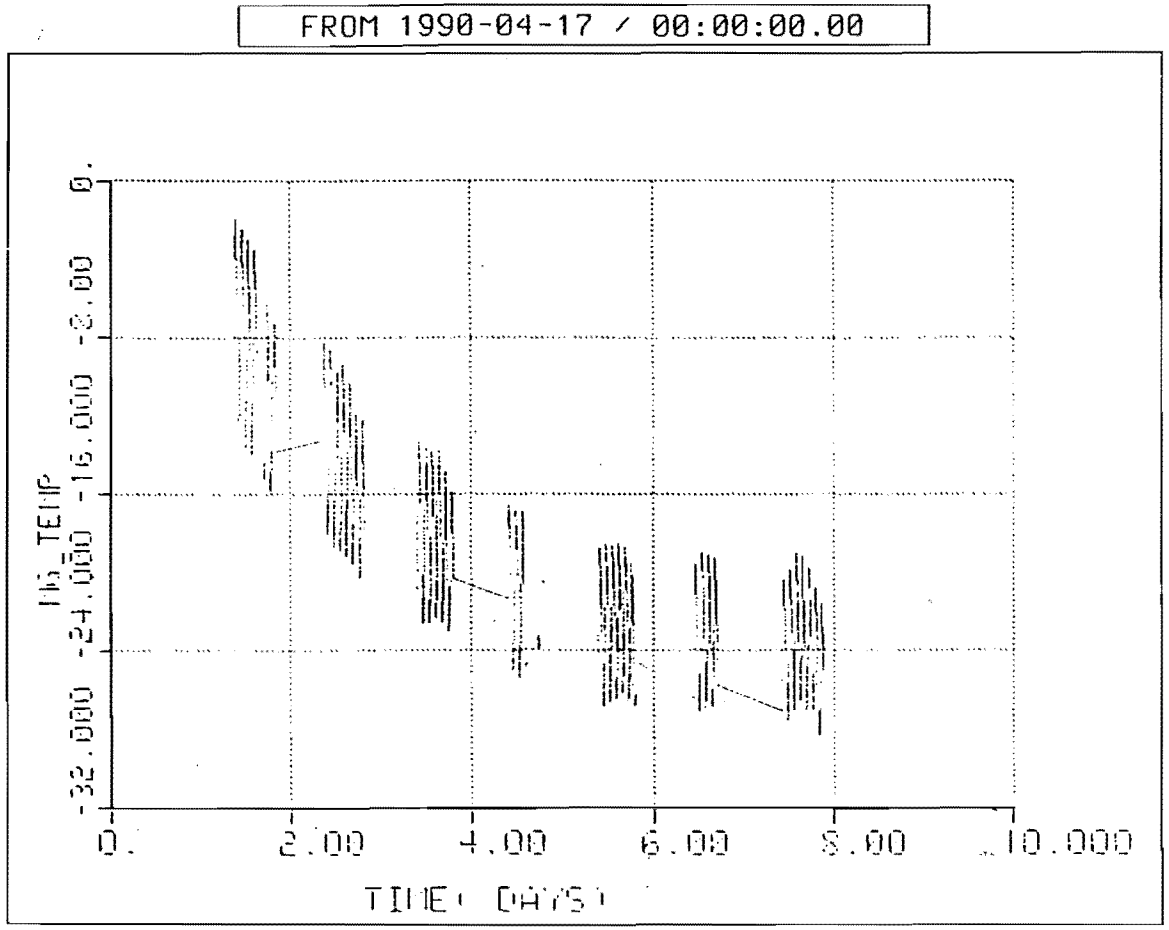
FROM 1990-04-17 / 00:00:00.00
-32.000
-24.000
-16.000
-8.00
0.
0.
2.00
4.00
6.00
8.00
10.000
TIME (DAYS)

FIGURE - 20

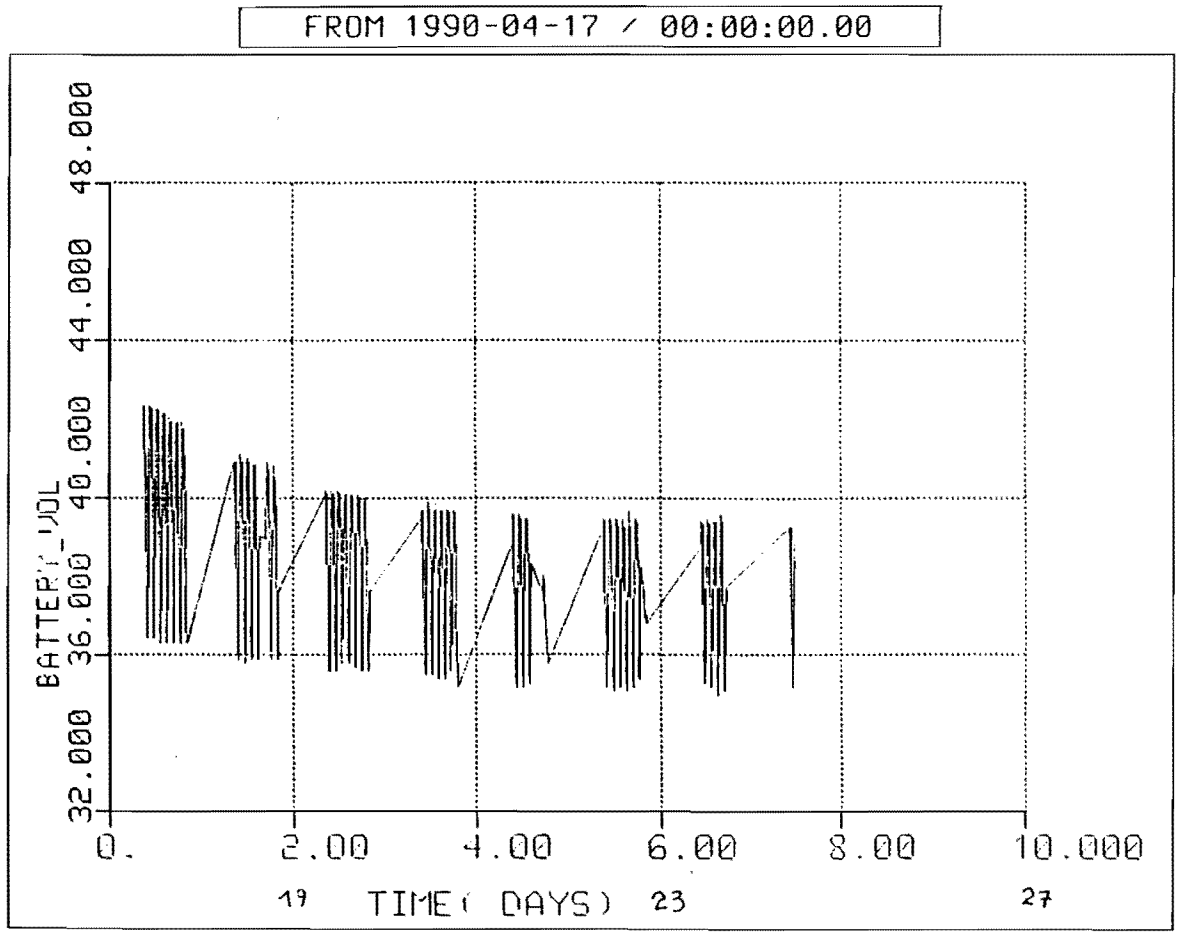

APRIL

FIGURE - 21

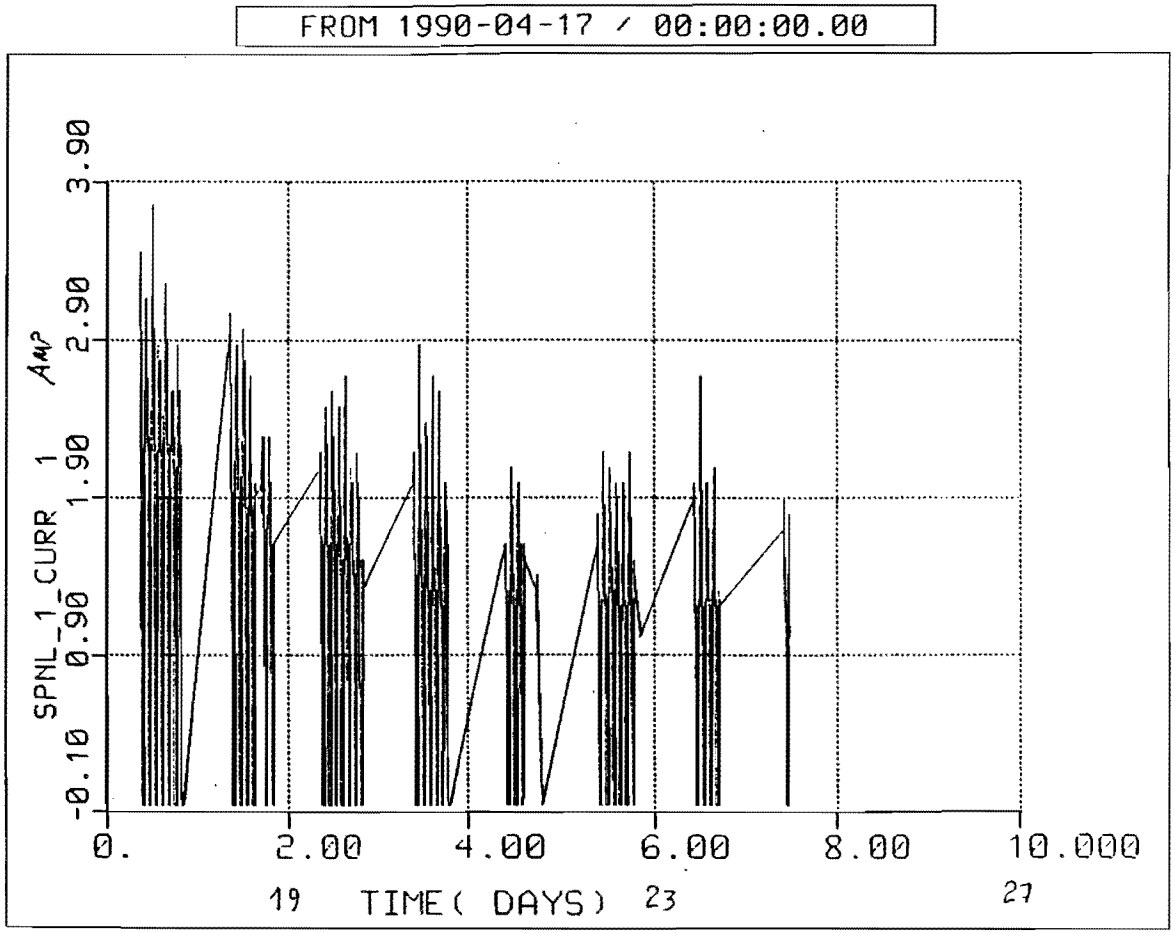

APRIL

FIGURE - 22

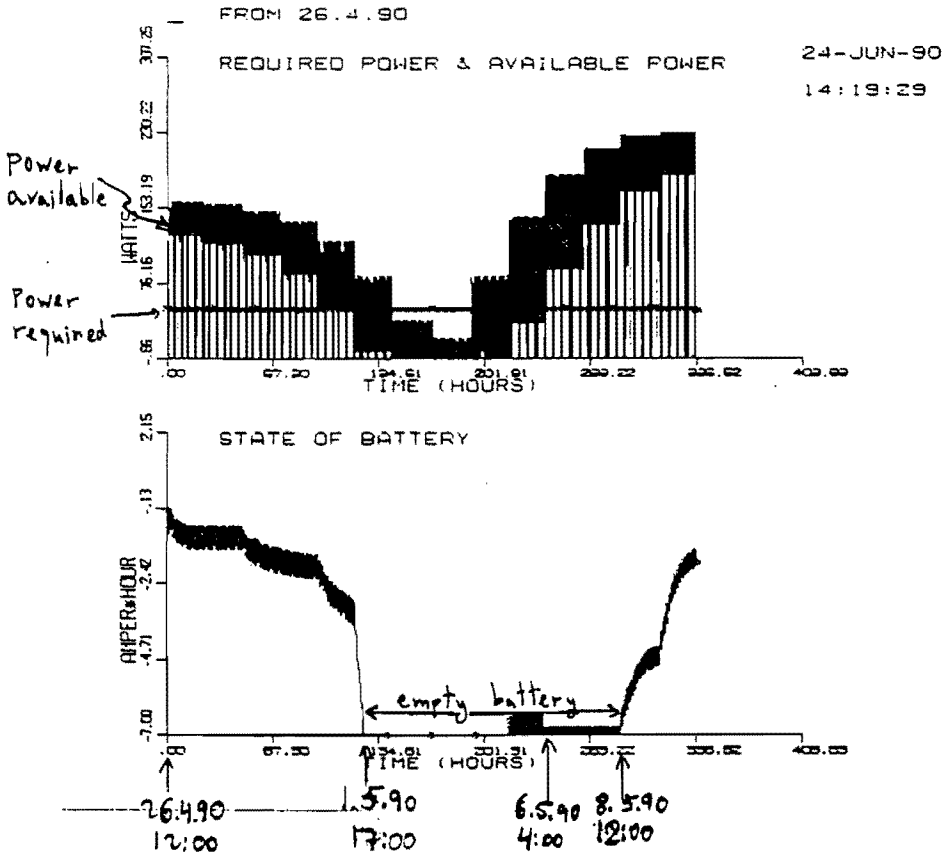
FROM 26.4.90
REQUIRED POWER & AVAILABLE POWER
24-JUN-90
14:19:29
Power available
Power required
WATTS
TIME (HOURS)
STATE OF BATTERY
AMPERE*HOUR
empty battery
TIME (HOURS)
26.4.90
12:00
1.5.90
17:00
6.5.90
4:00
8.5.90
12:00

FIGURE - 23

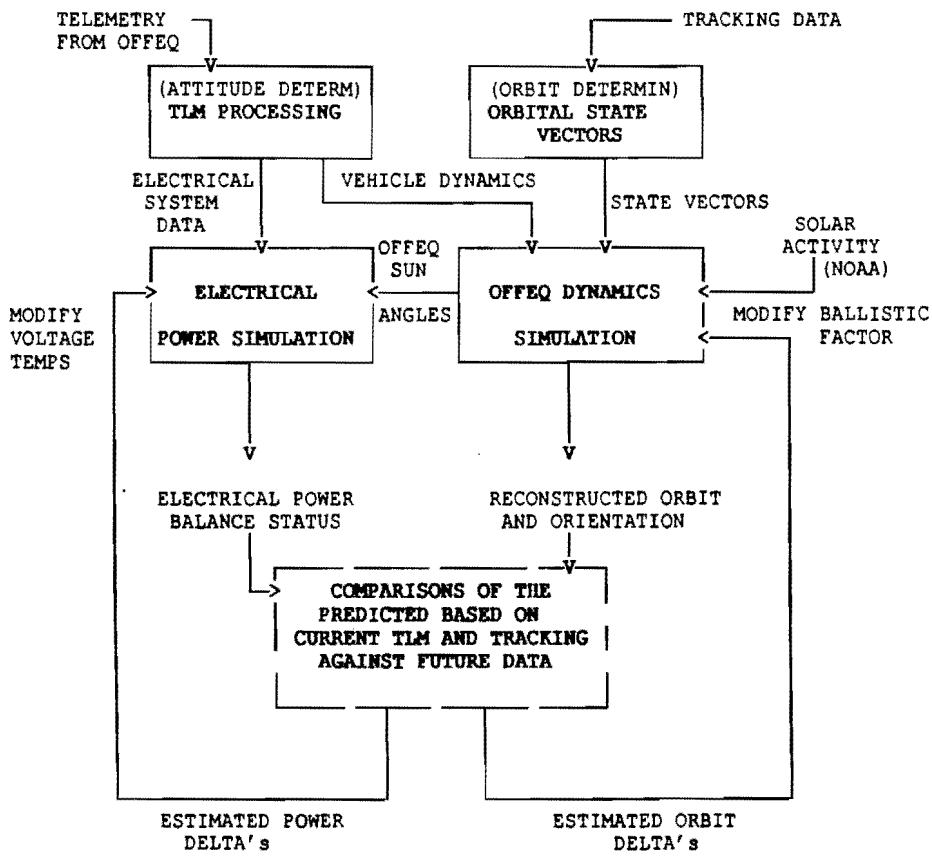

ORBIT AND ATTITUDE RECONSTUCTION PROCESS

Figure 24

Date	Time (UTC)	Latitude (Deg)	Longitude (deg)	Altitude (km)
4-April	1:21	- 19.2	-79.4	1,003*
4-April	9:21	- 25.4	-85.2	1,486*
7-April	9:08	- 25.3	-69.3	1,290*
12-April	8:38	- 35.4	-73.7	1,210*
24-April	19:22	34.8	-41.0	1,008

Table 3 Single Event Upset Summary

Note 1: Latitude Denoted - are south, longitude denoted - are west.

Note 2: A computer switch over occured on 10-April, 7:02 and located at -20 deg latitude, and -15 deg longitude.

YR	Mo.	DY.	CdFAC	FAVG	FDAY	Ap
1990	4	1	0.6	184.8	184.8	24.9
1990	5	1	0.6	186.8	186.8	17.6
1990	5	16	0.95	186.8	186.8	17.6
1990	6	2	0.945	168.8	168.8	16.0
1990	6	19	0.935	168.8	168.8	16.0
1990	6	23	0.865	168.8	168.8	16.0
1990	6	26	0.885	168.8	168.8	16.0
1990	6	28	0.86	168.8	168.8	16.0
1990	7	1	0.88	200.0	200.0	16.5
1990	7	6	0.925	200.0	200.0	16.5

TABLE 4: BALLISTIC FACTORS

#ORB	DOF	HTOT	DSPIN	DPRESS	DCON	DTRAN	KIN_ENG
15	1	197.71	367.89	124.27	0.478	1.04	634.73
64	4	195.29	363.38	122.75	0.640	1.38	619.29
76	5	196.21	365.10	123.33	0.646	1.40	625.17
123	8	194.65	362.17	122.35	1.020	2.21	615.19
137	9	195.11	363.00	122.64	1.130	2.45	618.02
154	10	194.66	362.14	122.36	1.300	2.80	615.14
185	12	194.76	362.28	122.42	1.650	3.57	615.68
200	13	195.12	362.91	122.65	1.820	3.93	617.85
229	15	193.82	360.40	121.83	2.250	4.82	609.46
242	16	193.68	360.07	121.74	2.470	5.30	608.42
260	17	192.53	357.87	121.02	2.700	5.74	601.06
275	18	192.90	358.43	121.25	3.090	6.59	603.10
288	19	191.87	356.44	120.61	3.360	7.13	596.51
293	19	192.28	357.16	120.86	3.430	7.29	598.96
308	20	192.48	357.40	120.99	3.790	8.06	599.95
323	21	191.53	355.49	120.39	4.130	8.74	593.69
337	22	192.01	356.19	120.69	4.520	9.58	596.27
353	23	191.93	355.83	120.64	4.950	10.48	595.29
368	24	191.58	354.89	120.42	5.440	11.50	592.47
383	25	190.83	353.21	119.95	5.910	12.43	587.22
399	26	191.04	353.23	120.08	6.470	13.64	587.71
415	27	190.52	351.83	119.76	7.070	14.86	583.55
430	28	189.75	349.98	119.27	7.610	15.92	577.94

TABLE 5A: ORIENTATION DATA BASED ON RATE GYROS

DYOFL	LATHI	LONHI	SPIN	TRANVL	CONANG	H2SUN	ANGMOM	PRECES
1.	-10.20	123.50	364.2	0.77	0.36	110.80	195.7	123.00
4.	-5.10	127.60	363.4	1.17	0.54	112.00	195.3	122.75
5.	-4.30	127.40	365.1	1.31	0.60	111.00	196.2	123.34
8.	18.20	144.07	362.2	1.93	0.89	119.03	194.7	122.35
9.	24.30	144.88	363.0	2.11	0.98	116.49	195.1	122.64
10.	37.20	147.91	362.1	2.45	1.14	111.74	194.7	122.35
12.	49.50	126.50	362.2	2.88	1.34	91.00	194.7	122.41
13.	62.96	115.50	362.9	3.40	1.57	81.00	195.0	122.64
15.	59.60	75.70	360.4	4.20	1.97	61.00	193.0	121.70
16.	49.60	69.70	360.0	4.46	2.10	52.10	193.6	121.71
17.	45.36	66.60	357.8	4.92	2.30	47.10	192.5	120.98
18.	31.77	73.40	358.4	5.53	2.60	45.30	192.8	121.20
19.	24.14	74.13	357.1	6.20	2.93	43.30	192.2	120.80
20.	21.74	75.27	357.4	6.86	3.20	43.14	192.3	120.92
21.	24.78	72.76	355.5	7.04	3.34	40.30	191.4	120.28
22.	23.83	72.83	356.2	7.82	3.67	39.30	191.8	120.57
23.	17.02	77.23	355.8	9.04	4.25	42.00	191.8	120.53
24.	12.51	76.76	354.9	9.97	4.73	40.92	191.4	120.29
26.	20.19	72.67	353.2	12.72	6.04	34.83	190.9	119.80
27.	22.82	67.78	351.8	11.90	5.68	29.60	190.0	119.98
28.	19.43	67.00	350.0	11.95	5.73	27.50	189.0	119.43

TABLE 5B: ORIENTATION DATA BASED ON MAGNETOMETER